

Experimental Study on Operational Effect of Wall-mounted Solar Air Collector (WSAC) by VAV Control

Xia Zhou^{1,2,a}, Gongxing Yan^{1,2,b,*}

¹*School of Intelligent Construction, Luzhou Vocational and Technical College, Luzhou, Sichuan, 646000, China*

²*Luzhou Key Laboratory of Intelligent Construction and Low-carbon Technology, Luzhou, Sichuan, 646000, China*

^a767509520@qq.com, ^byaaangx@126.com

*Corresponding author

Keywords: Wall-Mounted Solar Air Collector (WSAC), VAV, Transient Thermal Efficiency, Energy-Saving

Abstract: This study adopts the wall-mounted solar air collector (WSAC) as a research object, and experimental and theoretical studies were conducted. Specifically, this study proposed a strategy to improve operational efficiency based on the relationships of solar irradiance, supply air flow rate, WSAC transient thermal efficiency, and WSAC net efficiency. Moreover, under the VAV conditions, the building energy consumption was considered. Furthermore, this study analyzed WSAC thermal performance and energy-saving effect in an experimental room under constant, variable, and intermittent air supply volumes. The results show that the VAV air supply mode's net efficiency was more prominent than others considering the WSAC net efficiency. Moreover, compared to the constant air supply mode, the energy-saving rate was 63%. In addition, the best control operation mode was obtained with the changing solar irradiance.

1. Introduction

Wall-mounted Solar Air Collector (WSAC) is a flat-plate solar air collector that can be embedded in the building. Currently, domestic and international research on WSAC mainly focuses on optimizing the physical performance of WSAC, such as improving the heat transfer characteristics and their structure [1-4]. As the research and development of solar thermal utilization and integrated architect technology continues, optimizing control strategies for the heat transport process of building-integrated solar air heating systems attracted increasingly more attention. The following aspects have been typically studied: 1) control strategies to prevent cold air backflow [5]. 2) Optimization and control of the thermal transport system [6]. 3) Optimal combination control of WSAC mass flow and internal temperature rise [7]. The study [5] shows that WSAC effectively raises the room temperature under intermittent forced circulation via optimal control of the heat transfer process. However, the study did not propose a reasonable fan operating time and air supply

volume. On this basis, the paper [6] studied the relationship between heat supply and mass flow rate of an open-hole WSAC under mechanical air supply conditions based on various theories and experiments. The study [6] showed that the heat supply under the intermittent operation of the WSAC is higher than that under continuous operation. However, no control strategy is proposed for changes in the main influencing factors, such as solar irradiance and outdoor temperature. Subsequently, the study [7] investigated the intermittent control strategy of open-aperture WSACs. The results showed that the average thermal efficiency during WSAC operation was higher than the normal level, accompanied by more fluctuated room temperature. Moreover, due to the limitation of the fan air supply, the study [7] failed to obtain an optimal operating state point.

Based on the above research background, this paper uses a combination of experimental and theoretical analysis to investigate the variation of the transient efficiency of WSACs with solar irradiance and mass flow rate. This study also introduces the concept of pure efficiency to develop an in-depth discussion of the air volume control operational effectiveness of the open-hole WSAC under realistic outdoor climate conditions [11].

2. Experimental Methods

2.1 Experimental Facilities and Trial Methods

The experimental facilities are shown in Figure 1. The experimental room is about 9m². The WSAC is mounted on the wall between the windows on the south facade. The outer dimensions of the WSAC are 2044mm×540mm×120mm. The dimensions of the WSAC are 2044mm×540mm×120mm. The collector plate is located in the middle of the WSAC and is made of a 1mm thick through-hole 15-1 white steel plate with 5mm holes and a 15mm hole pitch. The surface of the white sheet is polished to increase the specific roughness. Moreover, the white steel plate is coated with a selective dark absorbance, of which the absorption rate is more significant than 0.9, and the emissivity is about 0.45 to 0.5.

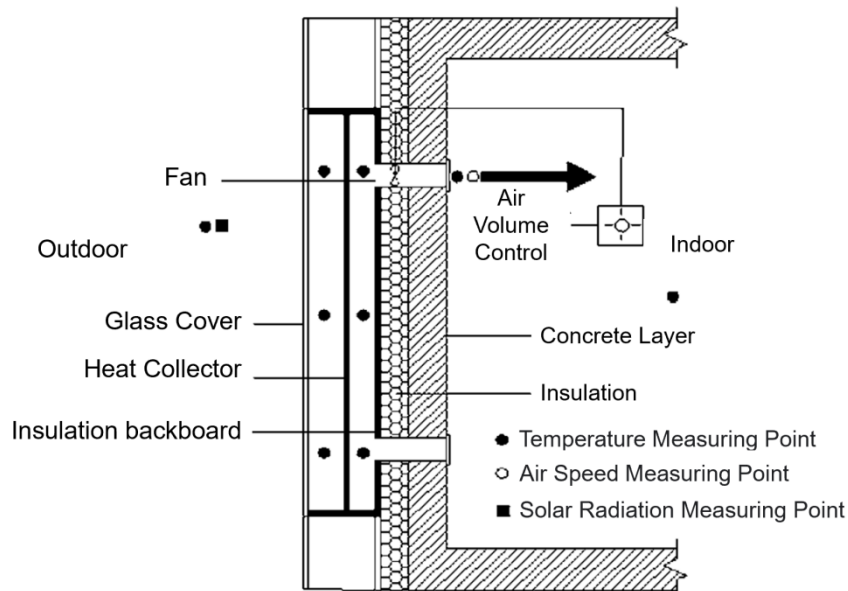


Figure 1: WSAC structure and measuring point arrangement

The WSAC is fitted with a centrifugal circular duct fan (Ck-100A) to connect to the room. The duct's diameter is 100mm. Its speed rate is 1730r/min, with a maximum airflow of 260m³/h. Also, the axis of the duct is 1.8m above the floor [12]. The WSAC can regulate the heat supply by

manipulating the fan airflow. Measurements were taken at the inlet and calibrated at the outlet using the log-linear method to ensure the accuracy of the trial. Thermocouple temperature measuring points were placed at different positions in the room to obtain precise indoor temperatures. We used sunshade tin foil to wrap the thermocouples to improve the accuracy of the test [13]. Moreover, corresponding measuring points were placed inside the WSAC and at the indoor side air outlets. The outdoor weather data (e.g., solar illumination, air temperature and humidity, wind speed, and direction) are collected using a PC-3 portable weather station with automatic roving. All data are automatically recorded by a computerized roving data collection system with 10 minutes intervals [14]. The experiment was conducted from January to March 2010.

2.2 Fan Performance Test Operating Conditions

This experiment focuses on the effect of implementing air supply regulation on optimizing the thermal performance of the WSAC, such as instantaneous thermal efficiency, pure efficiency, and heat supply [15]. The experiment can be divided into two phases. During phase 1, we examined the changing thermal performance of the WSAC under different air supply volumes. Then, in the second stage, the variable air supply performance of the WSAC was analyzed by selecting a reasonable air supply volume.

3 Experimental Results and Discussion

3.1 Analysis of WSAC Thermal Performance

3.1.1 Instantaneous Thermal Efficiency

The WSAC-regulated air supply volume is the volume of the fan at four consecutive calibrated positions, namely 43, 86, 105, and 154m³/h. The instantaneous thermal efficiency of the WSAC is calculated according to equation (1)[8].

$$\eta = \frac{mc_p (T_{out} - T_{in})}{AG} \quad (1)$$

Where η is the instantaneous thermal efficiency, G is the solar irradiance, W/m^2 , T_{out} and T_{in} are the air outlet and inlet temperatures of the WSAC, respectively, $^{\circ}C$, m is the air supply volume, kg/s , c_p is the specific heat capacity, $J/(kg-^{\circ}C)$, and A is the WSAC heat collection area, m^2 .

Figure 2 shows the WSAC instantaneous thermal efficiency variation with changing air supply under different solar irradiance. The instantaneous thermal efficiency of WSAC improves as the air supply volume increases. It can be seen that the instantaneous thermal efficiency increases as the air supply increases [16]. When the air supply increases to 154m³/h, the instantaneous thermal efficiency gradually decreases. The increase of instantaneous thermal efficiency decreases after the air supply volume increases to 154m³/h, which is more obvious in the case of higher solar illumination. Meanwhile, the greatest increase in instantaneous thermal efficiency of the WSAC is observed when the solar irradiance increases from 600W/m² to 650W/m². It shows that when the solar irradiance is greater than 600W/m², the instant thermal efficiency of WSAC can be significantly improved by increasing the air supply [17].

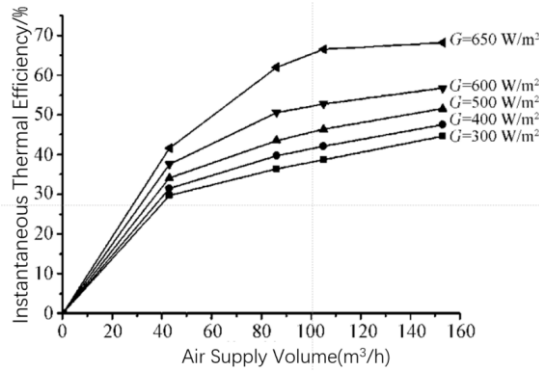


Figure 2: Variation of WSAC instantaneous thermal efficiency with supply air volume

3.1.2 Pure Efficiency

According to Fig.2, if the air supply volume has been increased to a certain value under the same solar irradiance, the instantaneous thermal efficiency change is insignificant if the air volume continues to increase [18]. At the same time, the large wind speed can increase electricity consumption. Thus, when studying the instantaneous thermal efficiency of the WSAC, the pure efficiency of the WSAC in the presence of fan power consumption should be considered. According to the study [9], the pure efficiency of WSAC as follows.

$$\eta' = \frac{mc_p (T_{out} - T_{in}) - P}{AG} \quad (2)$$

Where η' is the pure efficiency, P is the fan power, W and other parameters have been explained before.

According to the calculation formula (equation (3)) proposed in the study [10], the fan power, wind pressure, and speed can be calculated.

$$\frac{Q}{Q_m} = \frac{n}{n_m} = \left(\frac{P}{P_m}\right)^{1/3} = \left(\frac{\Delta p}{\Delta p_m}\right)^{1/2} \quad (3)$$

Where Q is the nominal air supply volume, m^3/h , Q_m is the nominal air supply volume, m^3/h , n is the fan speed at the nominal air supply volume, r/min , n_m is the nominal air supply volume, r/min , P_m is the rated power of the fan, W , Δp is the air pressure at the rated air supply, Pa , And, the rest of the parameters have been explained before.

Calculated via equation (3), the air pressure, power, efficiency, and power consumption per unit for air volumes of 43, 86, 105, and $154m^3/h$ are shown in Table 1.

Table 1: Fan parameters

Air Supply Q / (m^3/h)	Fan Pressure Δp / Pa	Power P / W	Efficiency η / $\%$	Unit Power Consumption / $(W/(m^3/h))$
154	119.1	8.5	60	5.5×10^{-2}
105	55.66	2.72	59.7	2.5×10^{-2}
86	40.48	1.48	59.8	1.7×10^{-2}
43	9.28	0.185	60	0.4×10^{-2}

The pure efficiency of the WSAC can be obtained via equations (2) and (3). The results are shown in Figure 3. The graph shows that when the air supply volume is small, there is no vital

difference between pure and instantaneous thermal efficiency [19]. The difference between pure and instantaneous thermal efficiency gradually increases with the increase in air supply. At a solar irradiance of $300\text{W}/\text{m}^2$ and an air volume is $154\text{m}^3/\text{h}$, the pure efficiency is 12.7% lower than the instantaneous thermal efficiency. In comparison, when the solar irradiance was increased to $650\text{W}/\text{m}^2$, the pure efficiency was 3.8% lower than the instantaneous thermal efficiency. Meanwhile, the decrease gradually decreased as the solar irradiance continued to increase [20].

From the above analysis, it can be seen that when the solar irradiance decreases to $300\text{W}/\text{m}^2$, a large air supply volume can reduce the pure efficiency of WSAC. Thus, it is appropriate to adopt $43\text{m}^3/\text{h}$ or $86\text{m}^3/\text{h}$ of the air supply volume. When the solar irradiance increases to $650\text{W}/\text{m}^2$ or more, a large air volume (e.g., $154\text{m}^3/\text{h}$) can result in relatively higher pure efficiency. However, when the air volume exceeds $154\text{m}^3/\text{h}$, there is no obvious improvement in pure efficiency when continues increasing the air volume. Therefore, changing air volumes can effectively improve the pure efficiency of the WSAC during the daytime.

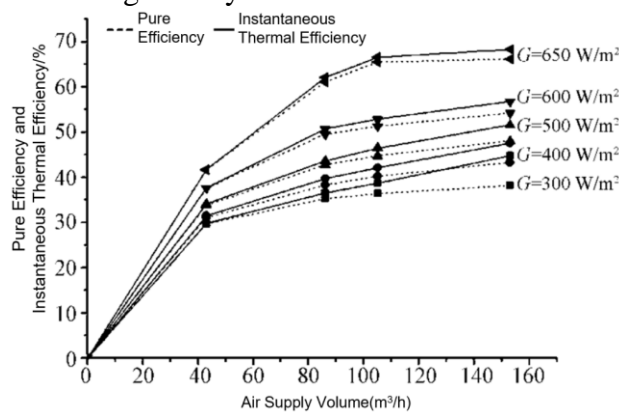


Figure 3: Variation of WSAC instantaneous thermal efficiency and pure efficiency with air supply volume

3.2 Variable air volume regulation

3.2.1 Operational Model

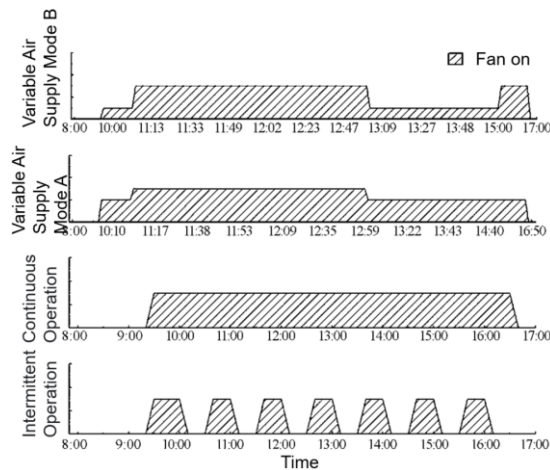


Figure 4: Variable air volume adjustment experimental conditions

To further understand the advances of variable air flow, this study comparatively investigated the instantaneous thermal efficiency and the heat supply of variable air supply, intermittent air supply, and continuous air supply. The four different experimental conditions are shown in Figure 4. Two

variable airflow models were designed based on the relationship between the WSAC pure efficiency, the air supply volume, and solar illumination.

When the solar irradiance is more significant than 300W/m^2 , the variable air supply mode A adopts an air volume of $105\text{m}^3/\text{h}$, and mode B takes an air volume of $43\text{m}^3/\text{h}$. This step aims to compare the effect of the air volume on the heat collection performance after smothering. When the solar irradiance exceeds 650W/m^2 , the variable air supply modes A and B adopt an air volume of $154\text{m}^3/\text{h}$. When the solar irradiance is below 500W/m^2 , the variable air supply modes A and B adopt $105\text{m}^3/\text{h}$ and $43\text{m}^3/\text{h}$, respectively. This compares the effect of supply air volume on the heat collection performance when the solar irradiance begins to weaken. When the solar irradiance decreases to 300W/m^2 , the variable air supply modes A and B adopt $105\text{m}^3/\text{h}$ and $154\text{m}^3/\text{h}$, respectively. This is to understand the influence of large air volume on heat collection efficiency under low solar radiation.

3.2.2 Study of the Effect of Variable Air Volumes on the Air Supply

Table 2 shows the operating parameters of the four operational situations. All parameters in the table are the average values from 7:00 to 17:00 of the day, and the power consumption is the cumulative value of the same time interval. It can be seen from the table that the continuous air supply with constant air volume has the highest average thermal efficiency. Moreover, the intermittent air supply has the worst average thermal efficiency. In addition, the variable air supply mode A has the highest average pure efficiency of WSAC. The key reason might be that with a constant air supply, the fan has been long-timely worked with an air volume of $154\text{m}^3/\text{h}$. However, the variable air supply mode A is an energy-saving mode set based on the relationship between solar irradiance, air volume, and pure efficiency. The power consumption of the latter is only 63% of that of the former.

Table 2: Thermal performance for different operating conditions

Operational Conditions	Average Thermal Efficiency %	Average Pure Efficiency %	Cumulative Heat Supply/kg	Power Consumption /kWh
Continuous Air Supply	0.69	0.676	10 786.2	0.0916
Intermittent Air Supply	0.408	0.408	9 464.84	0.0495
Variable Air Supply Mode A	0.687	0.679	11 007.5	0.0577
Variable Air Supply Mode B	0.457	0.451	7 214.04	0.0558

Figures 5 and 6 show the heat supply and instantaneous thermal efficiency of the WSAC in four operational situations. Combined with Table 2, that variable airflow mode A operates better than variable airflow mode B and continuous constant airflow. During the air supply phase, which starts after the WSAC has been sunburned; there is a significant increase in the instantaneous thermal efficiency and heat supply due to the large temperature difference between the inlet and outlet of the WSAC. This is why the average thermal efficiency in intermittent operation is 40.8%, which is lower than 45.7% of the variable air supply mode B., and the cumulative heat supply of the former is higher than the latter [22].

By analyzing the operation of two variable flow air supply modes, it can be found that there are two main reasons for the poor operating efficiency of mode B. Firstly, at the beginning of the operation, the air supply volume of WSAC was $43\text{m}^3/\text{h}$. Secondly, the air supply rate of WSAC was $154\text{m}^3/\text{h}$ when the solar illumination dropped sharply. WSAC was in the sultry phase before operating. The average internal temperature of the WSAC reached $50\text{ }^\circ\text{C}$ when the solar irradiance was below 500W/m^2 , which is approximately to be exposed to high solar irradiance. According to

the relationship between air supply and solar irradiance, it can be known that with high solar illumination, the low flow rate is not conducive to the thermal performance of the WSAC. The thermal performance of the WSAC in mode B, of which the air supply is $43\text{m}^3/\text{h}$, is worse than that of mode A[23]. Moreover, the air supply rate of mode B is as high as $154\text{m}^3/\text{h}$ when the solar illumination drops sharply in the afternoon. Again, according to the relationship between air supply and solar illumination, it can be known that this situation leads directly to a decrease in the pure efficiency of the WSAC.

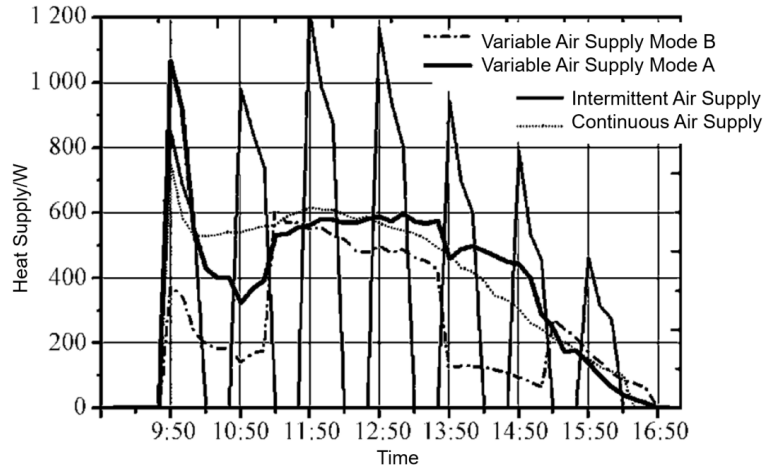


Figure 5: Comparison of heat supply under different operating conditions

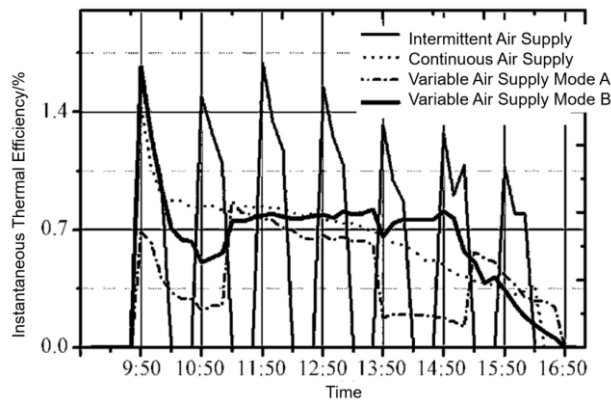


Figure 6: Comparison of instantaneous thermal efficiency of WSAC under different operating conditions

With variable flow rates, it is mainly the $154\text{m}^3/\text{h}$ that accounts for a smaller amount of the supply air time that consumes most of the power. Table 1 shows that the power consumption of the airflow at $154\text{m}^3/\text{h}$ is more than twice that of $105\text{m}^3/\text{h}$, while the air volume of the former is only 1.5 times of the latter. In addition, by comparing the initial stages of variable airflow mode A with continuous fixed airflow, the $105\text{m}^3/\text{h}$ and $154\text{m}^3/\text{h}$ airflows can make the WSAC's heating performance fully utilized during the initial stages of the WSAC's supply. This might result from the high internal temperature of the WSAC at that time. Thus, the excessive airflows cannot continually improve the WSAC's heat collection performance [21].

Therefore, in the initial stage of WSAC air supply, it is better to adopt an airflow of $105\text{m}^3/\text{h}$ for air supply. At noon, when the solar irradiance reaches the highest, it is better to use an airflow of $154\text{m}^3/\text{h}$. Also, in the afternoon, when the sun is about to set, the air supply should select an airflow of $43\text{m}^3/\text{h}$.

4. Conclusion

This study investigated the relationship between the air supply volume and the instantaneous thermal efficiency and pure efficiency of WSAC under different solar radiation illumination via experimental research and theoretical analysis. This study also analyzed the effect of optimizing the operation of WSAC by adjusting the air supply volume under different solar irradiance. The following conclusions were obtained [24].

Firstly, the instantaneous thermal efficiency increases with the increase of air supply, but the increase rate of instantaneous thermal efficiency decreases with the gradual increase of air supply. At the same time, the WSAC instantaneous thermal efficiency gradually increases as the solar radiation intensity increases.

Secondly, taking the fan's energy consumption into account, as the air volume increases, the difference between the pure efficiency and the instantaneous thermal efficiency of WSAC becomes more significant. When the solar irradiance is 300W/m^2 and the air supply is $154\text{m}^3/\text{h}$, the pure efficiency is 12.7% lower than the instantaneous thermal efficiency. When the solar irradiance is 650W/m^2 , the pure efficiency is only 3.8% lower than the instantaneous thermal efficiency.

Thirdly, considering the WSAC pure efficiency, the operating efficiency of variable air volume air supply is better than that of continuous constant air volume air supply and intermittent air supply. Moreover, the variable volume air supply mode A is 63% more energy efficient than continuous constant air supply.

Fourth, strategies to improve the operational efficiency of WSACs were obtained through the study. At the initial phase of the air supply after the WSAC has been smothered, the air supply should be at $105\text{m}^3/\text{h}$. Moreover, when the solar irradiance gradually reaches its maximum, the air supply should be at $154\text{m}^3/\text{h}$. In addition, when the solar irradiance drops to its lowest value, the air supply should be at $43\text{m}^3/\text{h}$.

Acknowledgements

This work was supported by Sichuan Province Luzhou city of Stars science and technology planning project (2022-GYF-16).

References

- [1] M. Chafe, M.F.B. Aissa, S. Bouadila, M. Balghouthi, A. Farhat, A. Guizani, *Experimental investigation of parabolic trough collector system under Tunisian climate: design, manufacturing and performance assessment*, *Appl. Therm. Eng.* 2016 (101): 273- 283.
- [2] M.T. JamalAbad, S. Saedodin, M. Aminy, *Experimental investigation on a solar parabolic trough collector for absorber tube filled with porous media*, *Renew. Energy*, 2017 (107): 156-163.
- [3] M. Valizade, M. Heyhat, M. Maerefat, *Experimental study of the thermal behavior of direct absorption parabolic trough collector by applying copper metal foam as volumetric solar absorption*, *Renew. Energy*, 2020 (145):261-269.
- [4] Y. Qiu, M.-J. Li, Y.-L. He, W.-Q. Tao, *Thermal performance analysis of a parabolic trough solar collector using supercritical CO₂ as heat transfer fluid under non-uniform solar flux*, *Appl. Therm. Eng.* 2017 (115): 1255 -1 265.
- [5] E. Bellos, C Tzivanidis, V. Belessiotis, *Daily performance of parabolic trough solar collectors*, *Sol, Energy* 2017 (158): 663- 678.
- [6] Lukic N. *The transient house heating condition the building envelope response factor (BER)*. *Renewable Energy*, 2003, 28(4):523~532.
- [7] Awbi HB. *Simulation of solar-induced ventilation*. *Renewable Energy Technology and the Environment*, 1992, 4:2016-2030.
- [8] Mao R.T. *Experimental study on the relationship between the performance of solar air heat collector module and the air flow rate*. *Solar Energy Journal*, 1989, 10(3):273-281.
- [9] Chen H.j., Chen B., Zhuang Z. *Calculation and Prediction of Heat Collecting Performance of Trombay Wall in Winter*. *Building Thermal Ventilation and Air Conditioner*, 2006, 25(2):1-6.

- [10] Chen B., Tian H., Guo H.C., etc. Study on the Best Heating Mode of Hanging Solar Air Heat Collector. *HVAC*, 2008, 38(10):128-132.
- [11] Chen B., Chen J. Operation control strategy of solar air heat collection building modules. *Solar Energy Journal*, 2010, 31(4):418-423.
- [12] Sun Y.F. *Research on optimal operation strategy of solar air heat collection modul*. Dalian: Dalian University of Technology, 2009.
- [13] Zhang H.F. *Principle of Solar Thermal Utilization and Computer Simulation*. Xian: Northwestern Polytechnical University Press, 2003:78~117.
- [14] IEA. *Solar Air Systems—A Design Handbook*. UK: James & James Ltd, 2000:201-212.
- [15] Wu Y.B. *Engineering Fluid Mechanics Pumps and Fans*. Beijing: Chemical Industry Press, 2006: 249~275.
- [16] Chuanzhang Zheng, Gongxing Yan, et al. Investigation of hyperbolic dynamic response in concrete pipes with two-phase flow. *Advances in Concrete Construction*, 2022, 13(5):361-365.
- [17] Gongxing Yan, et al. Using MHD free convection to receive the generated heat by an elliptical porous media. *Case Studies in Thermal Engineering*. 2022, 36(8):1-15.
- [18] Ji Min, Gongxing Yan, Azher M. Abed, Samia Elattar, Mohame, Amine Khadimallahd, Amin Jan, H. Elhosiny Ali. The effect of carbon dioxide emissions on the building energy efficiency. *Fuel*. 2022, 362(15):1-10.
- [19] Tang XZ (Tang, Xianzhi), Yan GX (Yan, Gongxing), ed at. Conventional and advanced exergy analysis of a single flash geothermal cycle. *Geothermal Energy*, 2022, 10(1):1-17.
- [20] Hao Wang, Gongxing Yan, Elsayed Tag-Eldin, ed at. Thermodynamic investigation of a single flash geothermal power plant powered by carbon dioxide transcritical recovery cycle. *Alexandria Engineering Journal*, 2022, (9):1-10.
- [21] Jingtao Sun, GongxingYan, ed at. Evaluation and optimization of a new energy cycle based on geothermal wells, liquefied natural gas and solar thermal energy. *Process Safety and Environmental Protection*. 2022, 168(10): 544-557.
- [22] Xie CG (Xie, Changgui), Yan GX (Yan, Gongxing), ed at. Flow and heat transfer optimization of a fin-tube heat exchanger with vortex generators using Response Surface Methodology and Artificial Neural Network. *Case Studies in Thermal Engineering*. 2022, 39 (10):1-13.
- [23] Shubo Zhang, Weiqin Jian, Jinglong Zhou, Jialing Li, Gongxing Yan, ed at. A new solar, natural gas, and biomass-driven polygeneration cycle to produce electrical power and hydrogen fuel; thermoeconomic and prediction approaches. *Fuel*. 2023, 334(2), 126824.
- [24] Gongxing Yan, BinTeng, ed at. Computational fluid dynamics simulation of a designed envelop contenting phase change material and imposed solar heat flux and ambient air. *Journal of Energy Storage*, 2022, 58(12): 106184.